J. Phys.: Condens. Matter **12** (2000) 7523–7539. Printed in the UK PII: S0953-8984(00)13201-1

Neutron diffraction study of the relaxor–ferroelectric phase transition in disordered $Pb(Sc_{1/2}Nb_{1/2})O_3$

C Perrin†, N Menguy†, E Suard‡, Ch Muller†, C Caranoni† and A Stepanov†

† Laboratoire L2MP—CNRS, Case 151, Faculté des Sciences et Techniques de Saint Jérôme, Université d'Aix-Marseille, III, F-13397 Marseille Cédex 20, France
and
Universite de Toulon, et du Var (UTV), BP 132, F-83957 La Garde Cédex, France
‡ Institut Laue Langevin, 6, rue Jules Horowitz, BP 156, F-38042 Grenoble Cédex 9, France

E-mail: perrin@matop.u-3mrs.fr and nmenguy@matop.u-3mrs.fr

Received 12 April 2000

Abstract. The crystal structure of chemically disordered lead scandium niobate, $Pb(Sc_{1/2}Nb_{1/2})O_3$, is studied by the high-resolution neutron powder diffraction method. The data, collected over the temperature range 2–653 K, are analysed using Rietveld refinement. From 653 K to 378 K, the symmetry of PSN is found to be cubic (space group $Pm\bar{3}m$) with positional disorder on the lead and oxygen crystallographic sites. For temperatures close to the ferroelectric phase transition (∼378 K), the formation of polar domains in the paraelectric phase is deduced from the observation of the diffuse scattering around Bragg peaks. For the ferroelectric phase, between 368 K and down to 2 K, the symmetry of PSN is determined to be trigonal (with space group $R3m$) and a positional disorder on the Pb site is evidenced perpendicular to the ferroelectric axis.

1. Introduction

The chemically disordered complex perovskite $Pb(Sc_{1/2}Nb_{1/2})O_3$ (hereafter D-PSN) belongs to the relaxor family. These materials exhibit a broad maximum and an unusual low frequency dispersion of their temperature dependent dielectric permittivity compared with regular ferroelectrics [1–4]. A common feature of these relaxor compounds is the existence of ferroelectric fluctuations in the paraelectric phase for temperature far above the temperature for which the maximum of dielectric permittivity is observed [4].

Among the different relaxor compounds, some of them exhibit no structural phase transition, like $PbMg_{1/3}Nb_{2/3}O_3$ (PMN) [5, 6], whereas some others exhibit a spontaneous relaxor–ferroelectric phase transition like $Pb(Sc_{1/2}Ta_{1/2})O_3$ or $Pb(Sc_{1/2}Nb_{1/2})O_3$ (PSN) [2, 7, 8].

Concerning stoichiometric D-PSN, a first order phase transition between the relaxor and the ferroelectric phases has been observed to occur at about 380 K by several authors [2, 3, 7, 9–11]. Structural data have been reported only for a few low and high temperatures (200 K and 400 K [9] or 10 K and 523 K [11]) with respect to T_c. In the ferroelectric state, disordered PSN phase has a rhombohedral structure (space group $R3m$) with displacements of the Pb atoms along the threefold axis which have been found to be larger than those of the Sc/Nb atoms. It has to be noticed that a significant discrepancy exists between the results reported in [9] and [11]; Knight and Baba-Kishi have reported an antiparallel displacement of

0953-8984/00/337523+17$30.00

Pb and Sc/Nb along the ferroelectric axis whereas Malibert *et al* have shown that Pb and Sc/Nb move in the same way. Moreover, a static positional disorder for lead and oxygen atoms has been shown to exist.

In the paraelectric state, disordered PSN is cubic with space group $Pm\bar{3}m$. A high value of the isotropic displacement parameter has been observed for lead atoms indicating the existence of a possible positional disorder, either static or dynamic [9]. Malibert and coworkers have shown that in the paraelectric state, lead atoms are shifted from their high symmetry position [11]. Such a behaviour of Pb has been previously reported for PMN [5, 6, 12] and may indicate the existence of polar domains in the paraelectric phase of D-PSN. For PMN, it was concluded from a fine study of the temperature dependence of the diffuse scattering that polar micro-regions with rhombohedral symmetry nucleate at about 600 K; the polar correlation length sharply increases at a temperature close to T_m ($\sim$270 K) and then reaches a maximum at about 200 K. This result on PMN has been recently confirmed from high resolution x-ray diffraction experiments by Dkhil [13].

Nevertheless, up to now, these polar clusters, which are known to play a fundamental role in the peculiar dielectric behaviour of these relaxor materials, have never been unambiguously observed for PSN.

Moreover, recent x-ray diffuse scattering studies performed on a disordered PSN single crystal have been interpreted in terms of ferroelectric (FE) and antiferroelectric (AF) ordering [14, 15]. A size effect due to the ionic size difference between the Sc^{3+} and Nb^{5+} ions and their disordering has been proposed to induce the existence of a local antiferroelectric ordering in the paraelectric phase. According to the authors of [14] and [15], the frustration between the FE and the AF ordering could be at the origin of the relaxor behaviour of disordered PSN. However, the model proposed by Takesue *et al* assumes an antiparallel displacement of Pb and Sc/Nb along $\langle 110 \rangle$ direction, which seems to be not in agreement with previous structural studies [9, 11].

The purpose of this work is a detailed study of the crystal structure of D-PSN as a function of temperature. We report results obtained from high resolution neutron powder diffraction data collected from 2 K up to 633 K. Particular attention has been turned towards the diffuse scattering detected above the transition temperature suggesting the existence of polar domains in the paraelectric state. The temperature dependence of the Pb and Sc/Nb atomic shifts and the mean-square atomic displacement factors of these cations are also discussed in connection with the results of Takesue *et al* [14, 15].

2. Experiment

2.1. Sample preparation

The wolframite precursor method was used to prepare the disordered $Pb(Sc_{1/2},Nb_{1/2})O_3$ powder [16]. Sc_2O_3 and Nb_2O_5 oxides were carefully mixed and calcined in a platinum crucible at 1550 K for 4 hours to form the $ScNbO_4$ precursor phase. The purity of the obtained $ScNbO_4$ phase was controlled using x-ray diffraction analysis. The $ScNbO_4$ phase was then mixed with PbO (with an excess amount of PbO equal to 2%) and calcined at 1270 K for 4 hours to obtain the $Pb(Sc_{1/2},Nb_{1/2})O_3$ powder.

The measured weight loss of the calcined PSN powder was smaller than 1%. A part of the powder was sintered following the way described by Stenger and Burggraaf [1] in order to perform electron microprobe analysis with wavelength dispersion spectroscopy (WDS). Analysis of several parts of the polished pellet of PSN led to the following chemical formula: $Pb(Sc_{0.48}Nb_{0.52})O_3$ with a precision better than 1%. Moreover, no evidence of the chemical

111 ordering between Sc and Nb atoms has been found from an x-ray diffraction experiment performed on the obtained powder.

2.2. Neutron diffraction experiments

Neutron diffraction experiments were performed on the high-resolution powder diffractometer D2B at the Institut Laue–Langevin (Grenoble, France) with an incident wavelength of 1.594 Å. The powdered PSN sample was sealed in a vanadium can and placed in dedicated furnace developed at the ILL. The D2B diffractometer is equipped with a bank of 64 ^{3}He detectors with 2.5° separation spanning an angular range of 160 degrees (2θ); a complete pattern acquisition is achieved by sweeping in steps of 0.05°. Two sets of data were collected: with a 6 hour counting time at 2 K, 300 K, 338 K, 353 K, 378 K, 433 K, 653 K and with a 2 hour counting time at 358 K, 368 K and 388 K.

Neutron diffraction patterns were analysed by the Rietveld method available in the program Fullprof [17]. The observed diffraction peak profiles were described using a pseudo-Voigt function with a refinable η parameter. The angular dependence of the full width at half maximum (FWHM) of the diffraction peaks was chosen to be of Caglioti type (e.g. $\mathrm{FWHM}(\theta) = (U\tan^2\theta + V\tan\theta + W)^{1/2}$ where U, V and W are refinable parameters) [18]. The background was adjusted from a five parameter polynomial function.

Systematic error corrections, such as zero-point and asymmetry of peak shape, were applied. The coherent scattering lengths used were $b_{Pb} = 9.40$ fm, $b_{Sc} = 12.29$ fm, $b_{Nb} = 7.05$ fm and $b_O = 5.80$ fm.

The structure proposed by Knight and Baba-Kishi [9] was taken as the starting crystallographic model for the ferroelectric rhombohedral phase (between 2 K and 368 K). The atomic positions are given in the non-centrosymmetric space group $R3m$ with a hexagonal cell.

Taking the Pb at the position $(0, 0, \frac{1}{2})$ and following the description given by Megaw and Darlington [19], the positions of the Sc/Nb and O atoms are described in terms of $z_{Sc/Nb} = 0 + \delta z_{Sc/Nb}$, $z_O = 1/6 + \delta z_O$ and $x_O = 1/6 \pm \delta x_O$. $\delta z_{Sc/Nb}$ and δz_O represent the atomic shifts from the ideal perovskite positions along the ferroelectric axis, i.e. the c axis, whereas the δx_O parameter describes the deformation of the oxygen octahedra.

For the high-temperature cubic phase (above 373 K), the atomic positions were given in the $Pm\bar{3}m$ space group, with reference to the ideal perovskite-type structure.

2.3. Transmission electron microscopy

Transmission electron microscopy (TEM) experiments were carried out using a Jeol 2010F electron microscope. The powder was crushed in a agate mortar and then deposited on a carbon film. Selected area diffraction patterns (SADP) were obtained using a very low excitation of condenser lens in order to avoid sample irradiation damage. A relatively long exposure time (up to 60 s) was also used in order to record diffraction patterns.

3. Results

3.1. Ferroelectric phase of D-PSN

High-resolution neutron powder diffraction diagrams collected at 2 K, 300 K, 338 K, 353 K and 368 K were fitted from the structural model described above. First, the scale factor and the instrumental parameters were refined. In a second step, atomic positions and individual isotropic atomic displacement parameters were refined with a Sc occupancy fixed to $x_{Sc} = 0.48$ according to the WDS results (with $x_{Sc} + x_{Nb} = 1$). When the Sc occupancy was refined, a

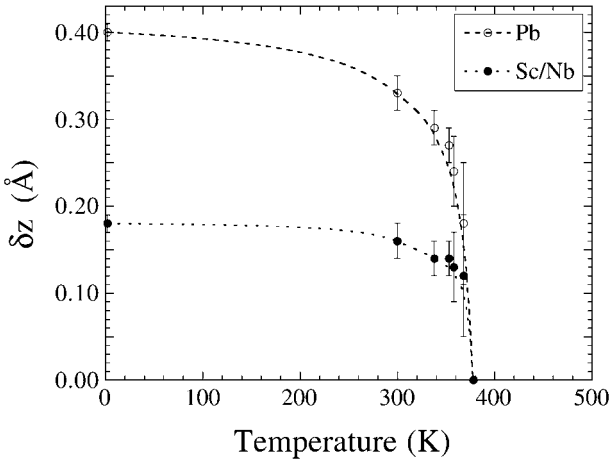

Figure 1. Temperature dependance of the cation shifts along the polar axis for the ferroelectric phase. The displacements are given with respect to the centre of the oxygen environment of each cation.

value in the range [0.36–0.41] was obtained with a significant diminution of the reliability factors, this phenomenon being observed whatever the temperature (e.g. in the ferroelectric state as in the paraelectric state). Furthermore, from x-ray powder diffraction data, the composition of the same powder was refined to $x_{Sc} = 0.48$ in agreement with the WDS analyses. The sample absorption correction, applied for all the structure refinements reported in this paper with $\mu r = 0.08$, does not improve the reliability factors and does not modify this unexpected occupancy. Moreover, the comparison between structural parameters obtained from the refinements performed for each temperature with respectively fixed or refined Sc occupancy systematically shows that:

(i) the atomic positions remain unchanged within the standard uncertainties;
(ii) the isotropic displacement parameters for Pb and O are smaller for $x_{Sc} = 0.48$ (fixed) than when x_{Sc} is refined;
(iii) the isotropic displacement parameters of the Sc/Nb pseudo-nucleus obtained with $x_{Sc} = 0.48$ (fixed) are closer to those reported by Malibert *et al* and Knight and Baba-Kishi and larger than those obtained when x_{Sc} is refined.

For these reasons, we have constrained the Sc occupancy to be equal to 0.48 for all the refinements reported in this paper. This anomaly of the Sc occupancy could be related to a static or dynamic displacement disorder on the B-site as recently described in the case of $PbHf_{0.4}Ti_{0.6}O_3$ [20] or on the A-site widely reported in Pb-based relaxors. A possible explanation will be discussed later.

With isotropic displacement parameters the refinements lead to satisfactory reliability factors, but when refinements are performed introducing anisotropic displacement parameters the R factors are significantly improved. Structural parameters are given in table 1. The temperature dependence of atomic shifts from the ideal perovskite positions for lead atoms and the Sc/Nb pseudo-nucleus is shown in figure 1.

For temperatures between 2 K and 368 K, the Pb and Sc/Nb nuclei move in the same direction with respect to the oxygen octahedron. These results are consistent with previous dielectric studies of D-PSN [1, 3, 7] and is in agreement with those obtained by Malibert *et al* [11] but not with those of Knight and Baba-Kishi [9].

Table 1. Structural parameters for the rhombohedral phase.

	2 K	300 K	338 K	353 K	358 K	368 K
Space group	*R*3*m*	*R*3*m*	*R*3*m*	*R*3*m*	*R*3*m*	*R*3*m*
a_h (Å)	5.7644(3)	5.7696(2)	5.7706(2)	5.7709(2)	5.7711(2)	5.7710(2)
c_h (Å)	7.0859(7)	7.0821(3)	7.0798(3)	7.0785(5)	7.0773(5)	7.0751(7)
a_r (Å)	4.0810(3)	4.0828(1)	4.0828(1)	4.0827(2)	4.0826(2)	4.0821(3)
α (°)	89.859(8)	89.915(4)	89.934(4)	89.943(6)	89.950(6)	89.962(8)
$z_{Sc/Nb}$	0.032(2)	0.030(1)	0.028(2)	0.027(2)	0.027(2)	0.025(3)
$x_O = 1/6 + \delta x_O$	0.1713(7)	0.170(1)	0.170(2)	0.169(2)	0.168(2)	0.168(3)
$z_O = 1/6 \pm \delta z_O$	0.221(4)	0.209(5)	0.205(4)	0.204	0.203	0.19(1)
B_{11}[Pb] (Å^2)	2.9(2)	3.5(3)	3.7(3)	3.7(4)	3.8(4)	3.9(7)
B_{33}[Pb] (Å^2)	0.5(3)	0.6(4)	1.0(6)	1.2(5)	1.4(6)	3(2)
B_{eq}[Pb] (Å^2)	2.1(3)	2.5(3)	2.8(4)	2.9(4)	3.0(5)	3(1)
B_{11}[Sc/Nb] (Å^2)	0.4(2)	0.4(3)	0.6(3)	0.5(4)	0.4(4)	1.0(7)
B_{33}[Sc/Nb] (Å^2)	1.1(3)	1.2(4)	1.2(5)	1.5(4)	1.6(5)	0.7(6)
B_{eq}[Sc/Nb] (Å^2)	0.6(2)	0.7(2)	0.8(3)	0.8(3)	0.8(3)	0.9(4)
B_{11}[O] (Å^2)	2.2(3)	2.0(3)	2.1(3)	2.2(5)	2.3(5)	2.4(7)
B_{22}[O] (Å^2)	0.6(3)	0.7(3)	0.8(3)	0.6(5)	0.7(5)	1.0(7)
B_{33}[O] (Å^2)	1.7(3)	3.1(3)	3.2(3)	3.2(5)	3.1(5)	3.5(7)
B_{eq}[O] (Å^2)	1.5(3)	1.9(3)	2.0(4)	2.0(4)	2.0(5)	2.3(7)
R_{wp} (%)	5.02	5.02	5.32	5.53	5.18	8.05
R_p (%)	3.81	3.84	4.06	4.21	5.40	6.07
χ^2	3.14	3.37	3.70	3.50	1.88	2.42
R_B (%)	2.68	2.35	2.73	2.60	3.01	3.51

$$R_{wp} = \left[\sum_i w_i(y_i - y_{ci})^2 \Big/ \sum_i w_i y_i^2\right]^{1/2} \qquad R_p = \sum_i |y_i - y_{ci}| \Big/ \sum_i y_i \qquad R_B = \sum_i |I_i - I_{ci}| \Big/ \sum_i I_i.$$

For anisotropic displacements, the exponent term takes the form

$$T = \exp[(-1/4)(\beta_{11}h^2a^{*2} + \beta_{22}k^2a^{*2} + \beta_{33}l^2a^{*2} + 2\beta_{12}hka^*b^* + 2\beta_{13}hla^*c^* + 2\beta_{23}klb^*c^*)]$$

$B_{eq} = (1/3)\sum_i B_i$ where B_i are obtained from the diagonalization of the $[\beta_{ij}]$ tensor.

The Pb displacement (0.40 Å at 2 K and 0.33 Å at 300 K) is similar to that obtained by Malibert *et al* (0.39 Å at 10 K and 0.28 Å at 300 K) and larger than the one obtained by Knight and Baba-Kishi (0.29 Å at 200 K) for PSN.

The displacement of the Pb atom along the threefold axis induces a noticeable deformation of the oxygen cubeoctahedron surrounding the Pb atom. Moreover, the oxygen octahedron is significantly distorted since at 2 K for the triangular faces perpendicular to the ternary axis, O–O distances are 2.78 Å for one face and 2.98 Å for the other one. At room temperature, these O–O distances are respectively 2.79 Å and 2.98 Å.

The Pb–O distances vary in the ranges 2.54–3.26 Å at 2 K and 2.59–3.20 Å at 300 K. It has to be noticed that the equivalent displacement parameter B_{eq}[Pb] is very high even at 2 K (2.1 Å^2) indicating the existence of a static positional disorder on the A-site in the ferroelectric state.

At 2 K, the displacement of the pseudo-atom Sc/Nb along the threefold axis with respect of the centre of the oxygen octahedron is 0.179 Å and becomes equal to 0.160 Å at 300 K which is consistent with the results of Malibert *et al* [11].

From the obtained values of anisotropic displacement parameters, it can be concluded that:

(i) the displacement ellipsoid of the pseudo-nucleus Sc/Nb is anisotropic and elongated along the threefold axis over the whole temperature range in the rhombohedral phase;

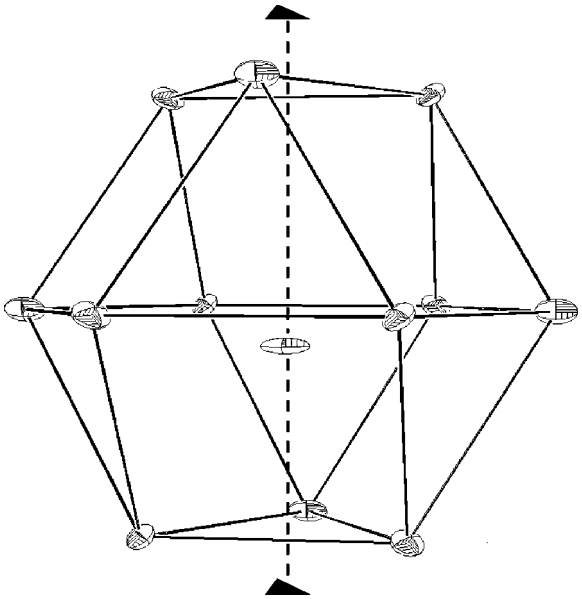

Figure 2. Pb environment with anisotropic displacement ellipsoids (ORTEP). The Pb displacement is clearly visible along the ferroelectric axis. The disc-shaped Pb displacement ellipsoid with the smallest axis parallel to the polar axis is also noticeable.

(ii) in the corresponding pseudo-cubic unit cell, the oxygen atoms are located at the centre of the faces and their displacement ellipsoids are flat and parallel to the faces of the pseudo-cubic cell;
(iii) the displacement ellipsoid of the Pb is a flat ellipsoid perpendicular to the polar axis.

The position of the lead atom seems to be relatively well defined along the polar axis but there is a positional disorder in the plane perpendicular to the polar axis (figure 2).

Disc-shaped anisotropic displacement ellipsoids for lead atoms have been already reported for PSN at low temperature [9, 11], for Zr-rich $PbZr_{1-x}Ti_xO_3$ [21], for $PbHf_{0.4}Ti_{0.6}O_3$ [20] and $PbHf_{0.8}Ti_{0.2}O_3$ [22].

3.2. Paraelectric phase of D-PSN

In table 2, the structural and atomic parameters of disordered $Pb(Sc_{0.48}Nb_{0.52})O_3$ from 378 K to 653 K are given according to the cubic space group $Pm\bar{3}m$. As for the rhombohedral phase, the Sc occupancy was fixed equal to 0.48. The ideal cubic perovskite structure assuming a regular oxygen octahedron leads to good results with correct R factors.

The most remarkable feature is the high value of the isotropic displacement factor B_{iso} of the Pb atom (4.5 Å^2) which is almost constant from 378 K to 653 K. This high B_{iso}[Pb] has been widely reported for lead-based complex perovskites such as PSN [9, 11], $PbMg_{1/3}Nb_{2/3}O_3$ [5], $PbMg_{0.3}Nb_{0.6}Ti_{0.1}O_3$ [13], $Pb(Fe_{0.5}Nb_{0.5})O_3$ [23] and for the $Pb(Hf_{1-x}Ti_x)O_3$ series [20, 22]. These anomalous isotropic displacement factors can be explained assuming the existence of static or dynamic positional disorder on the lead atoms. The 'split atoms' method may be used in order to reveal the existence of a preferential displacement direction of the lead atom from its ideal high-symmetry position [24]. This method has been performed for the paraelectric phase of D-PSN. For instance, at 388 K, it can be shown (figure 3(a)) that a shift of the lead atom along

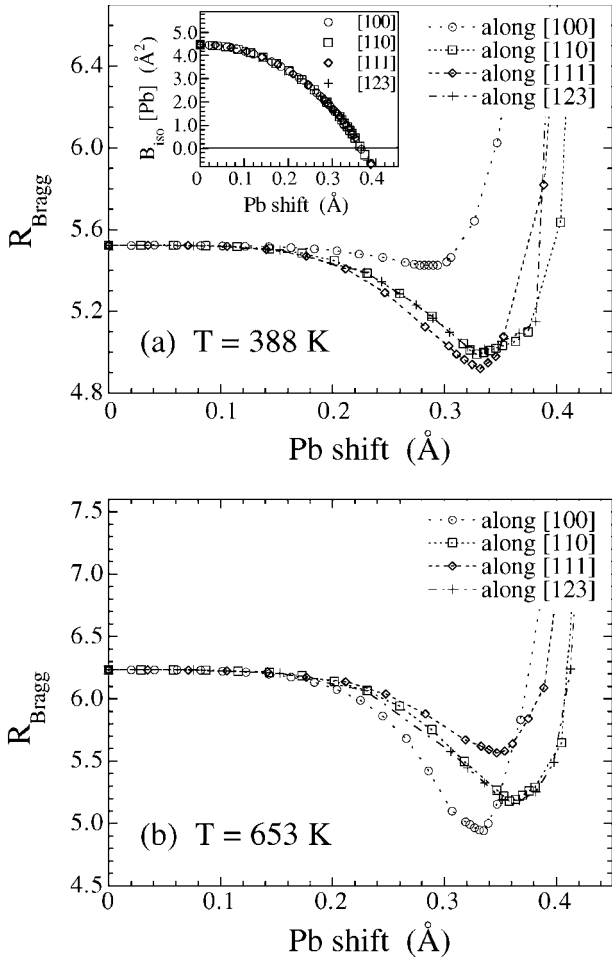

Figure 3. (a) R_B versus the Pb shift for the cubic phase of $Pb(Sc_{0.5}Nb_{0.5})O_3$ at 388 K. The model with Pb shift along $\langle 111 \rangle_{pc}$ directions shows a slightly deeper R_B-minimum than other models. The corresponding variation B_{iso} [Pb] as a function of the Pb shift is shown in the inset. (b) R_B versus the Pb shift for the cubic phase of $Pb(Sc_{0.5}Nb_{0.5})O_3$ at 653 K. The deepest R_B-minimum is obtained for the model with Pb shift along $\langle 100 \rangle_{pc}$ directions.

the $\langle 110 \rangle$, $\langle 111 \rangle$ and $\langle 123 \rangle$ directions leads to a significant decrease of the R_B factor with an important reduction of the B_{iso}[Pb] displacement factor to a more realistic value ($\sim$1 Å^2 instead of 4.39 Å^2). In contrast to this, a Pb shift along $\langle 100 \rangle$ directions does not induce a significant variation of the R_B factor. It is worth noting that a slightly deeper minimum is obtained for a displacement along a $\langle 111 \rangle$ direction. This result, obtained for 378 K, 388 K and 433 K, is connected with the Pb displacement along the threefold axis observed for the low temperature rhombohedral phase. However, such results have to be considered with great caution since it has been previously mentioned that a direction could be preferred with respect to others just as a consequence of a too small value of $(\sin\theta/\lambda)$ [23, 25]. At 653 K, a minimum in R_B is obtained with a displacement of Pb atoms along the $\langle 100 \rangle$ directions (figure 3(b)). These results clearly indicate that (i) in the paraelectric phase the lead atom position is fluctuating in a multi-minimum potential around the Wyckoff position and (ii) the multi-minimum potential changes with the temperature.

Table 2. Structural parameters for the cubic phase.

		378 K	388 K	433 K	653 K
Space group		$Pm\bar{3}m$	$Pm\bar{3}m$	$Pm\bar{3}m$	$Pm\bar{3}m$
a_c (Å)		4.0822(1)	4.0818(1)	4.0823(1)	4.0868(1)
[Sc/Nb] occupancy		$x = 0.48$ (fixed)	$x = 0.48$ (fixed)	$x = 0.48$ (fixed)	$x = 0.48$ (fixed)
With isotropic displacement parameters					
Pb	B (Å^2)	4.5(2)	4.5(2)	4.4(2)	4.5(1)
Sc/Nb	B (Å^2)	0.6(1)	0.7(1)	0.7(1)	0.89(5)
O	B (Å^2)	1.8(2)	2.1(1)	2.1(1)	2.42(6)
R_{wp}		7.62	8.87	7.25	5.6
R_p		5.49	6.69	5.16	3.47
χ^2		6.63	3.47	7.01	5.15
R_B		5.7	5.52	5.28	6.23
With anisotropic displacement parameters					
B_{eq}[Pb] (Å^2)		4.3(1)	4.4(2)	4.3(1)	4.4(1)
B_{eq}[Sc/Nb] (Å^2)		0.71(8)	0.78(8)	0.84(6)	1.00(7)
B_{11}[O] (Å^2)		0.86(5)	0.88(5)	0.82(4)	0.92(4)
B_{33}[O] (Å^2)		2.90(4)	2.88(4)	2.89(3)	3.32(3)
B_{eq}[O] (Å^2)		2.2(2)	2.2(2)	2.2(1)	2.5(1)
R_{wp}		6.23	7.85	5.66	6.27
R_p		4.55	5.95	4.23	4.64
χ^2		4.44	2.72	4.27	3.27
R_B		3.39	3.18	2.50	3.19

These results have been confirmed by direct refinements of Pb displacement. However, this method is less satisfactory because even with large damping factors, the value of R_B obtained this way is slightly higher than the one obtained by the split atom method. Moreover, it leads, in some cases, to unphysical negative values of the isotropic displacement factor.

When anisotropic oxygen displacement parameters were refined, the reliability factors drastically decreased. The resulting displacement ellipsoid is strongly anisotropic, with atomic displacement occurring mainly within the faces of the cubic unit cell (e.g. perpendicular to the Sc/Nb–O bonds) as for the rhombohedral phase.

3.3. Polar domains in the paraelectric state

In the case of disordered PSN, the relaxor behaviour and the existence of Pb positional fluctuations in the cubic phase suggest the existence of polar domains in the paraelectric state as reported in PMN. A structural refinement at 5 K was performed by de Mathan *et al* [6], using a two-phase Rietveld refinement with local polar regions (about 10 nm wide) inside a long-range cubic structure. According to these authors, the formation of polar regions results from correlation of atomic shifts along ⟨111⟩ cubic directions, leading to a local structure of trigonal symmetry. The most visible indication of the existence of these polar domains is the presence of diffuse scattering around some Bragg peaks. For PMN, at high temperature (800 K), no diffuse scattering is observed, the diffraction peak shape being almost Gaussian. When the temperature decreases, the diffuse scattering intensity around some peaks increases and the corresponding FWHM decreases. According to these authors, this phenomenon is due to the increase of the number and the size of the polar domains. These results have been recently confirmed by Dkhil for PMN and $PbMg_{0.3}Nb_{0.6}Ti_{0.1}O_3$ from x-ray powder diffraction experiments [13].

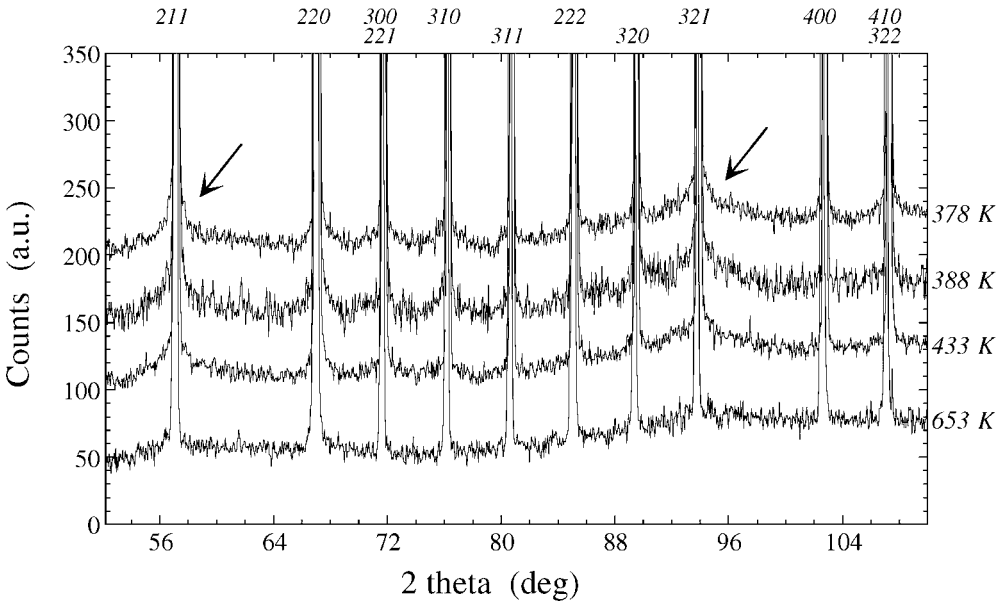

Figure 4. Evolution of the diffuse scattering observed around some Bragg peaks for different temperatures in the paraelectric state. At 653 K the peak shape is almost Gaussian; when the temperature decreases towards the paraelectric to ferroelectric transition temperature, the intensity of the diffuse scattering increases. *hkl* indices of the Bragg peaks are indicated at the top of the figure.

A careful examination of the background measured from our neutron diffraction experiments performed on disordered PSN in the cubic phase reveals the occurrence of diffuse scattering around some of the Bragg peaks as shown in figure 4.

Some similarities between the phenomena observed for PMN and PSN can be found:

(i) the Bragg peaks for which the diffuse scattering is observed are the same;
(ii) as the temperature decreases, the intensity of the diffuse scattering increases.

These findings give us some strong indications that the phenomenon in both materials has the same physical origin. It can be concluded that in disordered PSN, polar domains are growing in the paraelectric phase when the temperature is decreasing down to the first order cubic to rhombohedral phase transition. This result is in agreement with the observation of Takesue and coworkers [14, 15, 26] who have reported an increase in the ferroelectric fluctuations from the observation of an increasing of the diffuse scattering around the 300 reflection when the temperature decreases towards the phase transition temperature.

Attempts to measure the width and the intensity of the diffuse scattering in order to characterize more precisely the polar domains have been performed, but owing to the extreme weakness of the phenomenon, no polar domain size has been accurately determined.

3.4. Phase transition

The temperature dependence of the cell parameters is shown in figure 5. The observed evolution is very similar to the one reported for PSN by Malibert from x-ray diffraction experiments [10]. It has to be noticed that the evolution of the cell parameters does not exhibit a sharp variation as expected for a first-order phase transition.

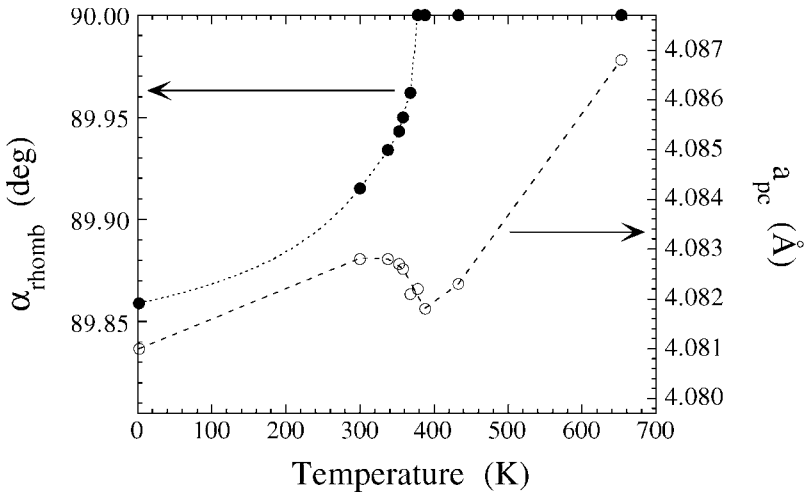

Figure 5. Temperature dependent evolution of the cell parameters given in the rhombohedral axes.

The temperature dependence of isotropic displacement parameters (figure 6(a)) shows that there is a sudden increase of atomic displacement factors upon entering the paraelectric phase (for the Sc/Nb pseudo-nucleus, the jump of the isotropic displacement factor is more visible in figure 7(b)). This result indicates that these are mainly lead and oxygen atoms which are involved in the paraelectric–ferroelectric phase transition. For lead atoms, figure 6(b) shows the thermal evolution of the atomic displacement factors $B_{\perp}$ ($=B_{11} = B_{22}$) and $B_{\parallel}$ ($=B_{33}$) respectively perpendicular and parallel to the polar axis for the ferroelectric phase and the displacement factor B_{eq} for the paraelectric phase. The augmentation of the parallel component $B_{\parallel}$ with increasing temperature indicates a enhancement of the positional disorder along the ferroelectric axis. In contrast, perpendicular to the polar axis, the disorder seems to be almost independent of temperature. Thus, for disordered PSN, the ferroelectric–paraelectric phase transition exhibits partially an order–disorder character.

For oxygen atoms, the evolution of anisotropic displacement parameters B_{ij} as a function of temperature shows that the displacement ellipsoid is a flat disc over the whole temperature range (not shown).

4. Discussion

4.1. Anomaly on the Sc/Nb site

For all temperatures, i.e. for both ferroelectric and paraelectric states, the refinement of the Sc occupancy x_{Sc} leads to a value lower than the expected one. Different hypotheses including existence of Sc or Nb vacancies on the B-site and substitution of Pb atoms on the B-site have been tested. A very slight improvement of the reliability factor has been obtained with a small amount of Sc vacancies on the B-site leading to the chemical formula $PbSc_{0.47}Nb_{0.50}O_3$. However a strong correlation between atomic displacement parameters and the site occupancy has been observed and this result may be not significant. Figure 7(a) shows the temperature dependence of the refined Sc occupancy. Figures 7(b), 7(c) and 7(d) display the temperature dependence of Sc/Nb, Pb and oxygen isotropic displacement parameters respectively for $x_{Sc} = 0.48$ (fixed) and for a refined occupancy. A significant variation of the Sc occupancy

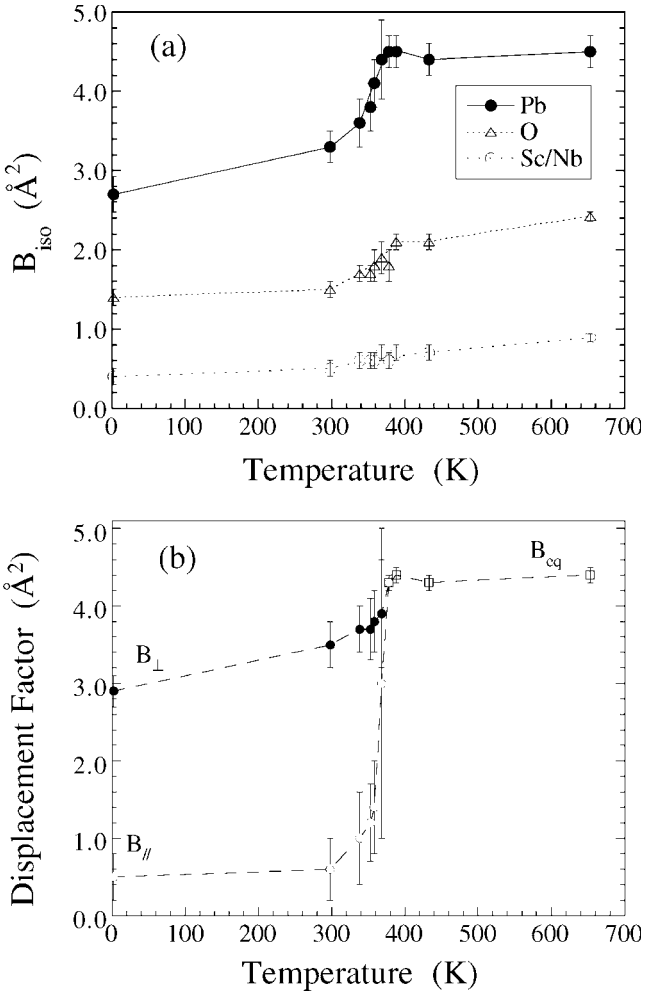

Figure 6. (a) Temperature dependences of isotropic displacement parameters of Pb, Sc/Nb and oxygen atoms. (b) Temperature dependences of the parallel and perpendicular components of the lead displacement ellipsoid with respect to the ferroelectric axis. For temperatures above 378 K, the variation of the equivalent displacement parameter for lead atoms is plotted.

can be seen in the vicinity of the phase transition temperature with a sudden jump of the isotropic displacement parameters. The variation of x_{Sc} with the temperature is not physically admissible and tends to invalidate the hypothesis of an anomalous stoichiometry on the B-site.

Moreover, concerning the Sc/Nb pseudo-nucleus, it has to be noticed that the refinement of x_{Sc} leads to two antagonistic consequences. On one hand, the decrease of x_{Sc} tends to minimize the contribution of the Sc/Nb pseudo-nucleus to the diffracted intensity and on another hand, the decrease of the isotropic displacement parameter B_{iso}[Sc/Nb] tends to increase this contribution. Furthermore, as previously mentioned, the influence of the Sc occupancy on the isotropic displacement parameters of lead and oxygen atoms is also clearly visible. Thus, it is possible to explain the unexpected low value of the refined x_{Sc} parameter as a consequence of the strong correlations between structural parameters.

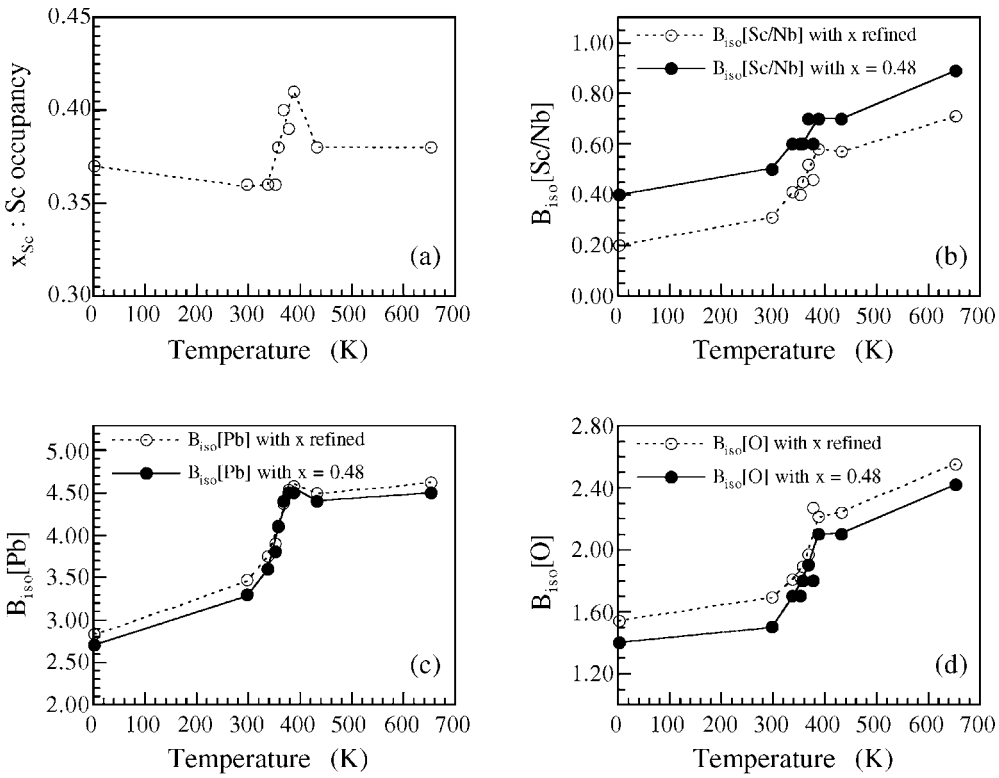

Figure 7. Temperature dependences of (a) the Sc/Nb occupancy and of the isotropic displacement parameter for (b) Sc/Nb, (c) lead and (d) oxygen when the Sc/Nb occupancy is refined or fixed.

In our opinion, this anomalous behaviour and the anisotropic displacement ellipsoid of the Sc/Nb pseudo-nucleus elongated along the polar axis in the ferroelectric state seem to reveal the existence of a positional disorder along the polar axis on the B-site.

Following the work performed on the $PbHf_{0.4}Ti_{0.6}O_3$ compound [20], for which a cationic splitting has been evidenced on the Hf/Ti site, some attempts have been carried out to separate Sc and Nb atoms (with constrained atomic displacement parameters and a fixed Sc occupancy equal to 0.48). The influence of an imposed shift δz between the two cations on the reliability factors was studied but no well marked minimum was observed. In a second step, atomic positions of the two cations were independently refined. However, no convergence with relevant and physically acceptable atomic parameters was obtained. Therefore, the positional disorder on the B-site is not due to a cationic splitting of the Sc/Nb site.

4.2. Disorder on the Pb site

The second point concerns the disorder on the Pb site existing in D-PSN over the whole studied range of temperature (2 K to 653 K). This disorder seems to be a common feature of numerous lead-based relaxors. For the ferroelectric phase, our neutron diffraction results reported in this paper show disc-shaped Pb displacement ellipsoids with the smallest axis parallel to the polar axis for temperature lower than 358 K.

From previous works on PMN [13, 27], PSN [9, 11], PST [28–31], PZT [21, 32] and $PbZrO_3$ [33], it appears that the physical origin of this apparent disorder could be a local

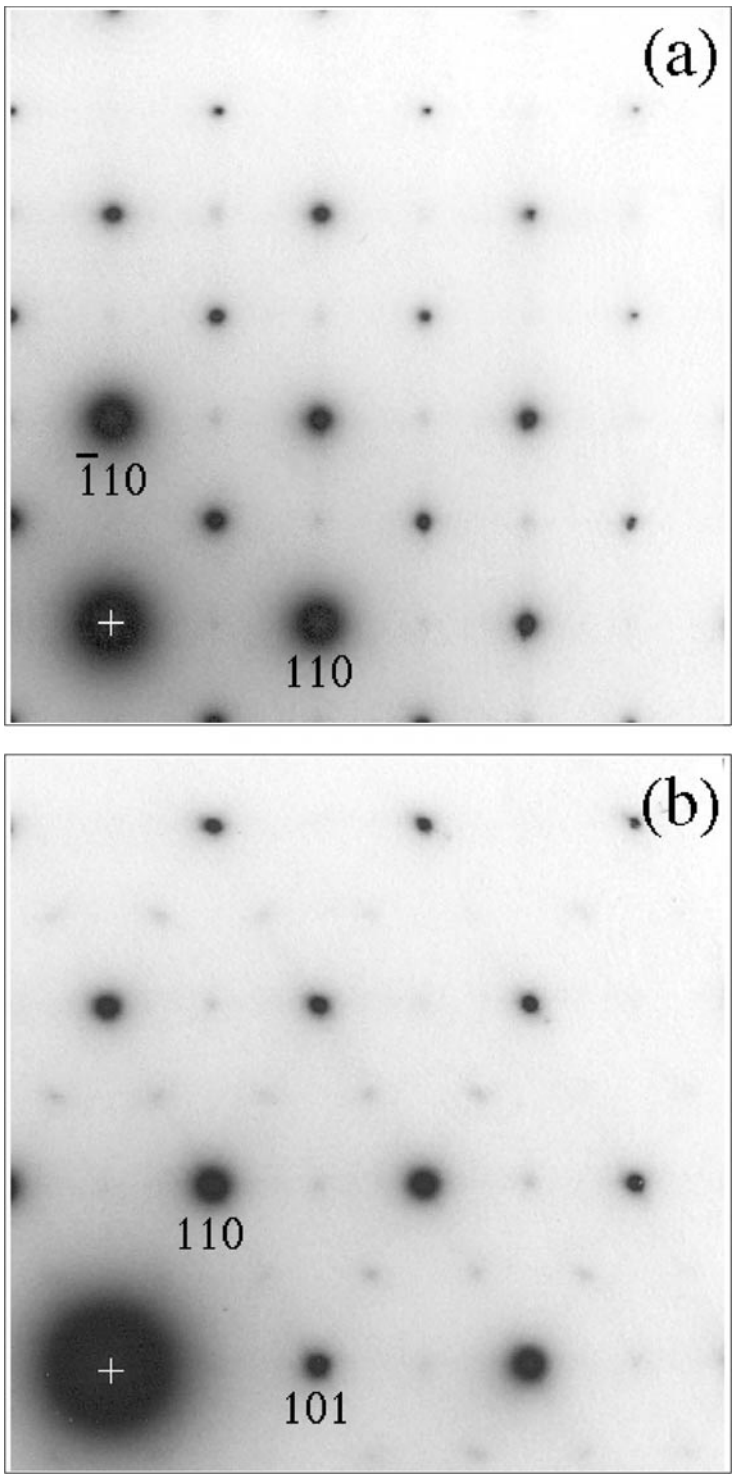

Figure 8. Selected area diffraction pattern of PSN obtained at room temperature along (a) [001] and (b) [$\bar{1}11$] zone axes respectively. Very weak ($h + 1/2\ k + 1/2\ 0$) reflections can be seen with diffuse scattering along $\langle 110 \rangle^*$ reciprocal directions.

ordering which can be evidenced using electron diffraction techniques. Figure 8 shows selected area diffraction patterns (SADPs) along $[001]_{pc}$ and $[\bar{1}11]_{pc}$ pseudo-cubic zone axes obtained at room temperature (e.g. in the ferroelectric state) on PSN particles. Diffuse streaks and very weak Bragg spots can be observed along the $\langle 110\rangle^*_{pc}$ reciprocal directions. The extra spots can be indexed as $(h + 1/2\ k + 1/2\ 0)$ in the pseudo-cubic cell description. The breadth of the spots indicates a short correlation length of a few cell parameters and their weakness denotes a very low degree of order. Owing to the weak intensities of these superstructure spots, it is not surprising that such reflections were detected neither by neutron nor by conventional x-ray diffraction at room temperature. It is worth noting that such superstructure reflections have been also observed by TEM at high temperature in the paraelectric state 200 K above T_c. Recently, in the case of PZT, Corker *et al* have proposed a multi-domain state with correlated displacements along $\langle 100\rangle_{pc}$ pseudo-cubic directions superimposed onto the $[111]_{pc}$ ferroelectric shift. According to Corker *et al* [21], the disc-shaped displacement ellipsoid obtained from the Rietveld refinement should be due to an averaging over the three $[100]_{pc}$ shifts of lead atoms. This extra ordering could lead to the appearance of extra reflections observed using electron diffraction by Ricote [32]. Following the procedure used by Corker *et al*, Pb atoms have been displaced from their high-symmetry positions $(0, 0, 1/2)$ to the one of the six equivalent $(x, y, 1/2)$ positions, thus allowing the Pb atoms to shift perpendicularly to the polar axis. In this way, the refinement converged easily for 2 K and 298 K with reliability factors better than with the lead in high-symmetry positions (with isotropic displacement parameter) but not as good as those obtained when anisotropic atomic displacement factors are refined. Moreover, no particular directions of the additional shift perpendicular to the ferroelectric axis can be unambiguously determined in this way, in contrast with the results obtained by Corker *et al*. Nevertheless, at 2 K and 298 K, the refinements provide realistic atomic displacement values ($\sim$0.2 Å, very close to the value obtained by Malibert *et al* [11] or Corker *et al* [21]) and confirm the existence of lead atom shifts perpendicular to the ferroelectric axis.

For 338 K and 353 K, improvements of reliability factors are not significant and for 358 K and 368 K, no convergence has been reached probably due to the strong correlations between the different refined parameters. However, these results are consistent with the temperature dependence of the anisotropic displacement parameters of lead atoms shown in figure 6(b): when the anisotropic character of the displacement ellipsoid disappears with increasing temperature, refinements with Pb atoms displaced from their high-symmetry positions become less relevant.

From our neutron diffraction results, it appears that no local ordering superimposed on the ferroelectric ordering has been unambiguously evidenced and these results could appear to disagree with electron diffraction observations and the results of Corker *et al*. However, it has to be noticed that the extra spots observed in the case of PSN are considerably weaker and more diffuse than the superstructure reflections observed by Ricote *et al*; it can be concluded that the domains corresponding to this extra ordering are smaller and fewer in PSN than in PZT. Moreover, it has to be pointed out that the Rietveld method is not able to describe properly the structure when there is short-range ordering. Nevertheless, our observation of disc-shaped displacement ellipsoids for Pb atoms and the existence of superstructure reflections by TEM are consistent with the results of Corker for which an extra ordering between Pb cations is assumed to exist.

On the other hand, our results are not consistent with the results of Takesue *et al* regarding the antiferroelectric ordering between Pb and Sc/Nb atoms [14, 15]. The discrepancy concerns mainly the Sc/Nb. In the model proposed by Takesue and coworkers, antiparallel displacements of Pb and Sc/Nb atoms are assumed to exist along $\langle 110\rangle_{pc}$ directions. The anisotropic

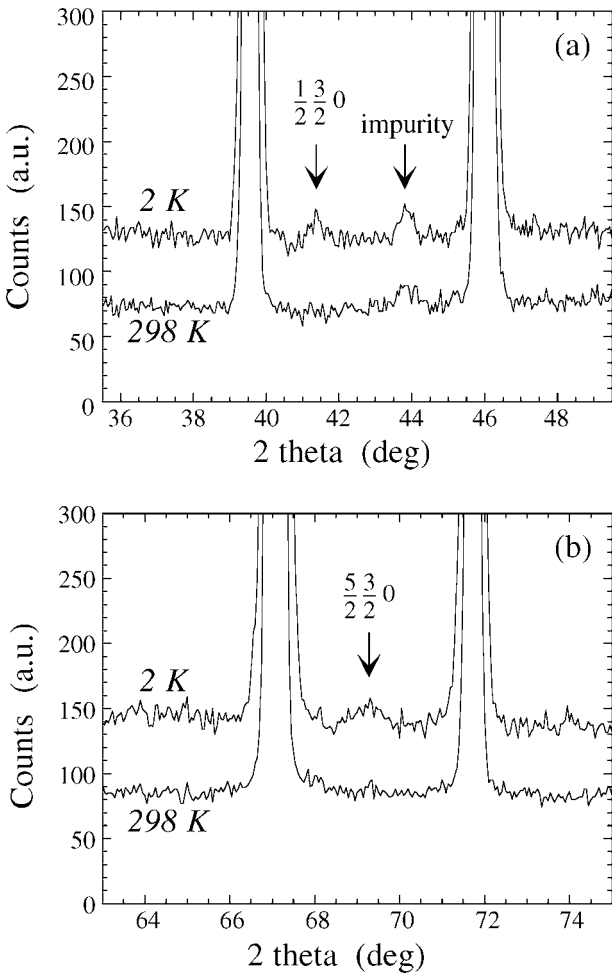

Figure 9. Comparison of two parts of the neutron powder diffraction pattern collected at 2 K and 298 K. Two weak peaks corresponding to a possible extra ordering of lead atoms (see text) can be seen on the 2 K pattern. The weak peak observed for both temperatures at 43.7° 2θ is due to a pyrochlore-type impurity.

displacement ellipsoid of Sc/Nb elongated along the polar axis in the ferroelectric state is not consistent with the hypothesis of Takesue *et al*. However, antiparallel displacements of Pb atoms such as proposed by Takesue are consistent with our results and with the existence of an extra ordering of Pb atoms.

A careful examination of the 2 K neutron diffraction pattern reveals the existence of very weak superstructure reflections that are not present at higher temperature as shown in figure 9. These very weak peaks can be indexed as $(\frac{1}{2}\ \frac{3}{2}\ 0)$ and $(\frac{5}{2}\ \frac{3}{2}\ 0)$ in the pseudo-cubic description and are consistent with the different extra orderings proposed by Corker *et al* for PZT, by Teslic and Egami for $PbZrO_3$ [33] and by Takesue *et al* for lead atoms in the case of PSN. Taking into account the particular shape of the displacement ellipsoid of oxygen atoms, the presence of in-phase octahedral rotations associated with the lead atom displacement could also be considered. The weakness of these superstructure reflections did not allow us to straightforwardly determine the nature of the corresponding ordering.

5. Conclusion

The ferroelectric–relaxor phase transition of disordered lead scandium niobate (D-PSN) has been investigated using neutron powder diffraction in association with Rietveld refinement in the temperature range 2–653 K.

At high temperature, in the paraelectric state, lead atoms are always displaced from their high-symmetry position. When the temperature decreases towards T_c, the correlation among Pb displacements along $\langle 111 \rangle_{pc}$ directions increases to form polar domains. At the transition temperature, 378 K, a long-range order rhombohedral phase, with $R3m$ space group, appears. This phase is characterized by the displacements of Pb and Sc/Nb atoms along the threefold axis with respect to the oxygen octahedron. A residual disorder has been found to exist for lead atoms and could correspond to an additional short-range ordering similar to one of those previously reported for lead-based complex perovskite.

The existence and the temperature dependence of the polar domains observed in the paraelectric phase of disordered PSN are in agreement with the relaxor behaviour of this compound.

Acknowledgments

The authors would like to thank the Institut Max von Laue–Paul Langevin (ILL), Grenoble, for allowing the neutron diffraction experiment to be carried out. We are grateful for the use of the Jeol 2010F TEM provided by the Centre Pluridisciplinaire de Microscopie et de Microanalyse (CP2M) at the University of Aix-Marseille III. We also gratefully thank Professor B Hilczer for useful discussion and F Robaud for EPMA analyses.

References

[1] Stenger C G F and Burggraaf A J 1980 *Phys. Status Solidi* a **61** 653–64
[2] Stenger C G F and Burggraaf A J 1980 *Phys. Status Solidi* a **61** 275–85
[3] Setter N and Cross L E 1980 *J. Mater. Sci.* **15** 2478–82
[4] Cross L E 1987 *Ferroelectrics* **76** 241–67
[5] Bonneau P, Garnier P, Calvarin G, Husson E, Gavarri J R, Hewat A W and Morell A 1991 *J. Solid State Chem.* **91** 350–61
[6] de Mathan N, Husson E, Calvarin G, Gavarri J R, Hewat A W and Morell A 1991 *J. Phys.: Condens. Matter* **3** 8159–71
[7] Chu F, Reaney I M and Setter N 1995 *J. Appl. Phys.* **77** 1671–6
[8] Chu F, Setter N and Tagantsev A K 1993 *J. Appl. Phys.* **74** 5129–34
[9] Knight K S and Baba-Kishi K Z 1995 *Ferroelectrics* **173** 341–9
[10] Malibert C 1998 *Thesis* Université de Paris 6
[11] Malibert C, Dkhil B, Kiat J M, Durand D, Berar J F and Spasojevic-de-Biré A 1997 *J. Phys.: Condens. Matter* **9** 7485–500
[12] de Mathan N 1991 *Thesis* Université de Paris 11 Orsay
[13] Dkhil B 1999 *Thesis* Université de Paris 11 Orsay
[14] Takesue N, Fujii Y, Ichihara M and Chen H 1999 *Phys. Rev. Lett.* **82** 3709–12
[15] Takesue N, Fujii Y, Ichihara M and Chen H 1999 *Phys. Lett.* A **257** 195–200
[16] Swartz S L and Shrout T R 1982 *Mater. Res. Bull.* **17** 1245–50
[17] Rodriguez-Carvajal J 1990 Fullprof. A program for Rietveld refinement and pattern matching analysis *Abstracts Satellite Meeting on Powder Diffraction XVth Congress Int. Union Crystallogr.* (Bordeaux: IUCR)
[18] Caglioti G, Paoletti A and Ricci F P 1958 *Nucl. Instrum. Methods* **3** 223–6
[19] Megaw H D and Darlington C N 1975 *Acta Crystallgr.* A **31** 161–73
[20] Muller C, Baudour J L, Madigou V, Bouree F, Kiat J M, Favotto C and Roubin M 1999 *Acta Crystallgr.* B **55** 8–16
[21] Corker D L, Glazer A M, Whatmore R W, Stallard A and Fauth F 1998 *J. Phys.: Condens. Matter* **10** 6251–69

[22] Muller C, Baudour J L, Bedoya C, Bouree F, Soubeyroux J L and Roubin M 2000 *Acta Crystallgr.* B **56** 27
[23] Lampis N, Sciau P and Geddo Lehmann A 1999 *J. Phys.: Condens. Matter* **11** 3489–500
[24] Itoh K, Zeng L Z, Nakamura E and Mishima N 1985 *Ferroelectrics* **63** 29
[25] Vakhrushev S, Zhukov S, Fetisov G and Chernyshov V 1994 *J. Phys.: Condens. Matter* **6** 4021–7
[26] Takesue N, Fujii Y, Ichihara M, Chen H, Tatemori S and Hatano J 1999 *J. Phys.: Condens. Matter* **11** 8301–12
[27] Egami T, Dmowski W, Teslic S, Davies P K, Chen I-W and Chen H 1998 *Ferroelectrics* **206/207** 231–44
[28] Baba-Kishi K Z and Barber D J 1990 *J. Appl. Crystallgr.* **23** 43–54
[29] Baba-Kishi K Z, Gressey G and Cernik R J 1992 *J. Appl. Crystallgr.* **25** 477–87
[30] Randall C A, Barber D J and Whatmore R W 1987 *J. Microsc.* **145** 275–91
[31] Reaney I M, Barber D J and Watton R 1992 *J. Mater. Sci.* **3** 51–63
[32] Ricote J, Corker D L, Whatmore R W, Impey S A, Glazer A M, Dec J and Roleder K 1998 *J. Phys.: Condens. Matter* **10** 1767–86
[33] Teslic S and Egami T 1996 *Acta Crystallgr.* B **54** 750–65